論文 / 著書情報
Article / Book Information

Title	Study of carrier energetics in ITO/P(VDF-TrFE)/pentacene/Au diode by using electric-field-induced optical second harmonic generation measurement and charge modulation spectroscopy
Authors	Takako Otsuka, Dai Taguchi, Takaaki Manaka, Mitsumasa Iwamoto
Citation	Journal of applied physics, 121, , 065501/1-6
Pub. date	2017, 2
Note	This article may be downloaded for personal use only. Any other use requires prior permission of the author and AIP Publishing. The following article appeared in Journal of applied physics, 121, , 065501/1-6 and may be found at http://dx.doi.org/10.1063/1.4975484.
Note	This file is author (final) version.

Study of carrier energetics in ITO/P(VDF-TrFE)/ pentacene/Au diode by using electric-field-induced optical second harmonic generation measurement and charge modulation spectroscopy

Takako Otsuka, Dai Taguchi, Takaaki Manaka, and Mitsumasa Iwamoto*

Department of Physical Electronics, Tokyo Institute of Technology,

2-12-1, O-okayama, Meguro-ku, Tokyo 152-8552 Japan

Abstract

By using electric-field-induced optical second harmonic generation (EFISHG) measurement and charge modulation spectroscopy (CMS), we studied carrier behavior and polarization reversal in ITO/ poly(vinylidene fluoride trifluoroethylene) (P(VDF-TrFE))/pentacene/Au diodes with ferroelectric P(VDF-TrFE) layer in terms of carrier energetics. The current-voltage (*I-V*) characteristics of the diodes showed three-step polarization reversal in dark. However, the *I-V* was totally different under illumination and exhibited two-step behavior. EFISHG probed the internal electric field in the pentacene layer and accounted for the polarization reversal change due to charge accumulation at the pentacene/P(VDF-TrFE) interface. CMS probed the related carrier energetics, and indicated that exciton dissociation in pentacene molecular states governed carrier accumulation at the pentacene/ferroelectric interface, leading to different polarization reversal processes in dark and under light illumination. Combining EFISHG measurement and CMS provides us a way to study carrier energetics that govern polarization reversal in ferroelectric P(VDF-TrFE)/pentacene diode.

Keywords: poly(vinylidene fluoride trifluoroethylene); ferroelectric polymer; electric-field-induced optical second-harmonic generation; charge modulation spectroscopy

---

*Corresponding author

Tel/Fax: +81-3-5734-2191

Email: iwamoto@pe.titech.ac.jp

1. Introduction

Since the discovery of conducting organic materials, organic devices have attracted much attention in electronics [1,2]. Their attractive features include good mechanical flexibility, light weight, ease of device fabrication based on solution process, and so forth. A lot of organic devices have been developed, among them are organic field effect transistors (OFETs), organic memory devices, organic diodes, etc [3]. These devices make use well of the attractive features of organic materials by employing organic semiconductors as active layers of organic devices. Organic semiconductors possess wide energy gaps and rather low intrinsic carrier densities [4]. Consequently, their device operation is governed by carriers injected from electrodes [5]. In other words, the electrical property of organic semiconductors is dielectric-like [6,7]. On the basis of this idea that organic materials exhibit the dielectric property, we have developed a method for analyzing organic devices as Maxwell-Wagner (MW) effect elements [8-12]. According to the MW effect, excess charges accumulate at the interface between adjacent two layers with different relaxation times, ε/σ [13]. Here ε and σ are the dielectric permittivity and conductivity, respectively. The analysis showed that the MW effect well accounts for the transfer characteristics of organic devices such as OFET, that is, carriers injected from the source electrode are accumulated at the interface between active layer and gate insulating layer due to the MW effect and they are then transported along the OFET channel [10,14,15]. It was

suggested that one of important parameters for fruition of innovative organic device function is to control the amount of charges at the interface. Since then, many research groups have been paying attention to use ferroelectric materials in organic devices [16,17]. Spontaneous polarization will be induced in ferroelectric layer, and an internal electric-field is accordingly generated in the active layer of the device. Recently, OFETs with ferroelectric gate insulator have been investigated for the development of nonvolatile memory devices [18-21]. Also, it has been reported that the incorporation of ferroelectric layer into organic solar cells is effective for enhancing the efficiency of the solar cells [17]. However, it is still not clear the details of the effect of the ferroelectric materials on the carrier behaviors in organic devices. This motivated us to study the relationship between the polarization reversal and the charge behaviors in the active layer, by using metal/ferroelectric layer/semiconductor/metal (MFS) diodes and OFETs with ferroelectric layer.

As the first step, we here focus on MFS diodes. Displacement current measurement (DCM) and capacitance-voltage (C-V) measurement are the conventional techniques used for analyzing the carrier behaviors in metal/insulator /semiconductor/metal (MIS) diodes [22]. For analyzing MFS diodes with ferroelectric layer, the DCM and C-V measurements are available in the same way, though we need to consider the effect of spontaneous polarization of the ferroelectric layer on the accumulation of charges at the interface between the ferroelectric layer and the active

layer. In other words, the carrier injection, accumulation and transport processes in MFS diodes are complex, in comparing with these in MIS diodes.

The DCM and C-V characteristics of MFS diodes can be obtained experimentally but these measurements are no longer sufficient to get detailed information of the carrier behaviors in the diodes, where a turn-over of spontaneous polarization happens in the ferroelectric layer during measurements. In measurement of MFS diodes, both of carrier behavior in semiconductor layer and polarization reversal in ferroelectric layer contribute to electrical current, and lead us difficult to extract carrier behaviors from the electrical current by using equivalent circuit and simulation. We therefore have been developing a method of electric-field-induced optical second-harmonic generation (EFISHG) measurement that can probe carrier behavior in a selected layer of organic multilayer systems [6,23]. In our previous study, by combining the DCM with EFISHG measurement we discussed the interaction of interfacial charges and ferroelectric polarization in MFS diodes [24-26]. Results showed that accumulated charges at the interface make a significant contribution to the polarization reversal of the ferroelectric layer, and the presence of different polarization reversal processes was found, depending on experimental procedures, e.g., under illumination and in dark [27]. However, we cannot make clear the details from view point of carrier energetics. Main reason is that we can observe carrier behaviors in MFS diodes by using EFISHG, but we cannot get energetic information on these

carriers. In other words, we need to see molecular energy levels that are responsible for these carrier behaviors.

Charge modulation spectroscopy (CMS) can probe carrier energetics, reflecting the nature of molecular energy states [28,29]. In this study, we freshly coupled CMS with EFISHG and DCM to study clear carrier energetics that related to polarization reversal of MFS diode.

2. Experimental

Figure 1a shows the structure of ITO/ poly(vinylidene fluoride trifluoroethylene) (P(VDF-TrFE))/pentacene/Au diodes. The devices were prepared as follows; P(VDF-TrFE) (70-30 mol.%) copolymer powder was first dissolved in methyl-ethyl-ketone solvent (concentration: 5 wt%), and P(VDF-TrFE) layer (thickness: 200 nm) was spin-coated on the glass substrates with a patterned ITO transparent electrode, followed by annealing in a dry nitrogen atmosphere at 120 ℃ for 1 h. Subsequently, a pentacene layer (thickness: 200 nm) and an Au electrode (thickness: 100 nm) were successively deposited by vacuum evaporation, where the process pressure and deposition rate were set $<10^{-5}$ Torr and 1 Å/s, respectively. The device area was approximately 3 mm^2.

DCM was employed using the electrical circuit illustrated in Fig. 1a. A ramp voltage generated from a function generator (NF, WF1974) and then amplified with a power amplifier

(NF, HSA4101) was applied onto the ITO electrode with reference to the Au electrode. The amplitude and frequency of the ramp voltage were 60 V and 5 mHz, respectively.

The EFISHG measurement was carried out by applying a ramp voltage in the manner same as in the DCM. Figure 1a shows the experimental setup for the EFISHG measurement. A laser pulse was generated from the third-order harmonic light of a Nd:YAG laser (Continuum, SureliteII-10) and an optical parametric oscillator (Continuum, Surelite-OPO). A p-polarized fundamental light was focused on the device from the ITO electrode side with an incident angle of 45° to detect the electric field formed along the film thickness direction. The generated EFISHG was selectively detected by a photomultiplier tube (PMT) after eliminating the probing laser by using optical filters. EFISHG is a third-order nonlinear process, and its intensity is given as [30]

$$I_{2\omega} \propto |\boldsymbol{P}_{2\omega}|^2 \propto \left|\varepsilon_0 \chi^{(3)} \vdots \boldsymbol{E}_0 \boldsymbol{E}_\omega \boldsymbol{E}_\omega\right|^2, \qquad (1)$$

where ε_0 is the vacuum permittivity, $\chi^{(3)}$ is the third-order susceptibility, $\boldsymbol{E}_0$ is the electrostatic field and $\boldsymbol{E}_\omega$ is the electric field of the incident laser beam. It is worth noting that $\chi^{(3)}$ has wavelength dependence and it is unique to the material. In this study, we used incident laser light with a wavelength of 860 nm and the second-harmonic (SH) light generated at $\lambda = 430$ nm from the pentacene layer was monitored [31,32]. The generation of an SH signal from ITO and P(VDF-TrFE) is negligible at $\lambda = 430$ nm. The electrostatic field in the layers of

double-layer structure diode is well described by using Maxwell-Wagner effect model as illustrated in Fig. 1b [33]. In pentacene/P(VDF-TrFE) diode, electrostatic field $E_1(=E_0)$ in Eq. (1) is formed from electrode charges Q_e, interfacial charges Q_s, and spontaneous polarization P and it is expressed as [34]

$$E_1 = \frac{1}{d_1}\frac{C_2}{C_1+C_2}V_{ex} + \frac{1}{d_1}\frac{Q_s}{C_1+C_2} + \frac{1}{d_1}\frac{P}{C_1+C_2} \quad (2)$$

where C_1(=0.74 nF) and C_2(=1.0 nF) are capacitance of pentacene and P(VDF-TrFE) layer, d_1 is the pentacene layer thickness, and V_{ex} is external voltage applied. By using Eqs. (1) and (2), we can obtain interfacial charges Q_s that govern turn-over of polarization in ferroelectric layer. Both DCM and EFISHG measurements were carried out in dark and under light illumination. White light emitting diode ($10\ \mathrm{mW/cm^2}$) was used for the illumination.

On the other hand, CMS is a technique which probes the modulated optical spectrum of the device in response to the change of the energetic structure induced by carrier injections. Accordingly, we can identify molecular energy states that involves in accumulation of interfacial charges Q_s. Figure 1c shows the experimental setup for the CMS [35]. A white light from a halogen lamp (intensity $\approx 1\ \mathrm{mW/cm^2}$) passed through an objective microscope lens, and was focused onto the device at a perpendicular angle from the ITO electrode side. The spot area was 40 μm in diameter. The reflected light was gathered with a monochromator (Andor Technology: SR-163) attached to a cooled charge-coupled device image sensor (Andor

Technology: DU-920P- BV) over a range of wavelength between 400 nm to 920 nm. The relative change in the reflection spectrum ($\Delta R/R = (I_\lambda - I_{\lambda 0})/I_{\lambda 0}$) was measured with the device biased from -60 V to +60 V, and $I_{\lambda 0}$ is the reference spectrum. The reference spectrum was the reflection spectrum at -60 V in the process from negative to positive voltage region (-60 V→ +60 V) and at +60 V in the process from positive to negative voltage region (+60 V→ -60 V).

3. Results and Discussion

3.1 DCM and EFISHG

Figure 2a shows DCM results. Two peaks (peaks A and B) are clearly observed at symmetric positions of applied voltages V(=V_A, V_B) with respect to $V = 0$, both in dark and under light illumination. In the positive voltage region, another peak (peak C) is observed at a higher voltage (V=V_C) only in dark. These three peaks originate from spontaneous polarization reversal of the P(VDF-TrFE) layer and produce hysteresis loops in the negative and positive voltage regions. In our previous studies, we showed that peak A is a displacement current peak due to the polarization reversal, which accompanies hole injection from the Au electrode to pentacene, followed by hole accumulation at the pentacene/P(VDF-TrFE) interface [24, 36]. Similarly, peak B is the displacement current peak due to the polarization reversal, and it

happens when the pentacene layer is in a conductive state. The peak C is assigned to the displacement current due to the polarization reversal, and it happens when the pentacene layer is in a non-conductive state. These results suggested that illumination eliminated peak C due to increased conductivity of pentacene layer.

Figure 2b illustrates the EFISHG result which probes electric field in pentacene layer. In the positive voltage region (V>0), in dark condition, electric field in the layer increased after polarization reversal at V_B=+15V, as external voltage increases. At the external voltage $V = V_B$, electric field in P(VDF-TrFE) layer E_2 = 0.85 MV/cm is obtained by using the relationship $V = E_1 d_1 + E_2 d_2$ (d_2: P(VDF-TrFE) layer thickness) and electric field in pentacene layer E_1 from the EFISHG measurement. The value of E_2 (= 0.85 MV/cm) is in good agreement with that we reported previously [24]. The electric field saturates after V=V_C where pentacene switches to conductive state due to electron injection from Au electrode. On the other hand, under illumination, the electric field saturates after V=V_B. The result indicates that pentacene is conductive under illumination, and electrostatic potential is only formed across the P(VDF-TrFE) layer. These results support the idea that the illumination enhanced conductivity of the pentacene layer and eliminated the polarization reversal at peak C in the DCM measurement. Figure 2c illustrates interfacial charges Q_s under illumination obtained from the EFISHG measurement. In the forward voltage sweep from V= -60 V to +60 V, accumulated

holes are released from the interface with keeping the relation $\Delta Q_s = C_2 \Delta V$, and at V=V_B, holes are totally decayed and electrons are accumulated in accordance with the polarization reversal of the P(VDF-TrFE). After that, electrons are smoothly accumulated with the relation of $|\Delta Q_s| = C_2 \Delta V$. In the same way, in the backward sweep from V=+60 V to -60 V, electrons are released from the interface until the polarization reversal at V=V_A. Afterwards, holes are accumulated to complete the loop. Note that we plotted absolute density of charges $|\Delta Q_s|$ to discuss carrier behavior in coupling with CMS in section 3.2.

As mentioned above, peaks observed in the DCM are different in dark and under light illumination, indicating that the polarization reversal at higher voltage (peak C) only appears in dark. Results obtained by the DCM and EFISHG measurements suggested that the photoconductivity of pentacene governed the polarization reversal at higher voltage region, but relationship between occupation of molecular orbitals and the polarization reversal in the P(VDF-TrFE) layer is still not clear in terms of carrier energetics. To further investigate photogenerated carrier behaviors under illumination, we probed carrier energetics in the pentacene/P(VDF-TrFE) diode by using CMS.

3.2 CMS

Figure 3 shows the results of CMS measurement for the ITO/P(VDF-TrFE)/pentacene/Au

diode. Changes of the reflection spectrum were measured in the forward direction measurement from -60 V to +60 V, where the spectrum at $V = -60$ V was chosen as the reference spectrum (Fig. 3a). In the same way, the spectrum at $V = +60$ V was chosen as the reference spectrum in the backward direction measurement from +60 V to -60 V (Fig. 3b). In Figs. 3a and 3b, the relative changes of the reflection spectra $-\Delta R/R$ were displayed. Noteworthy, $-\Delta R/R > 0$ represents the increase of absorption, whereas $-\Delta R/R < 0$ represents the decrease. Figure 4a shows optical absorption spectrum of pentacene film. Pentacene film has strong absorption peaks at wavelength of 540 nm, 580 nm, 630 nm and 670 nm in the visible light region whereas P(VDF-TrFE) is optically transparent over the visible light region. The absorption peaks correspond to electronic excitation between relevant molecular energy states. That is, the peaks at 540 nm (E1: 2.30 eV) and 580 nm (E2: 2.14 eV) are due to the HOMO-LUMO excitation, and the peaks at 630 nm (E3: 1.97 eV) and 670 nm (E4: 1.85 eV) are due to Davydov components [37-40]. Figures 4b-4e plot relative optical modulation $-\Delta R/R$ at the wavelength corresponding to these absorption peaks. The results showed that different molecular states contribute in a different way according to polarization reversal in the diode. The optical modulation $-\Delta R/R$ at 540 nm and 580 nm (Figs. 4b and 4c) exhibit butterfly-like loop which is symmetric in respect to V = 0 V. This behavior closely links to carrier behavior at the pentacene/P(VDF-TrFE) interface shown in Fig. 2c. Under illumination, excitons are created

due to optical transition between HOMO and LUMO (E1 and E2 in the inset of Fig. 4a). The created excitons are dissociated into free holes and electrons, and these are a direct source of interfacial charges Q_S. The dissociated excitons cannot contribute to radiative recombination, and cause increase of absorption ($-\Delta R/R>0$) in proportion to interfacial charges Q_S. This situation makes clear an origin of free carriers in dark and under illumination in the diode for turn-over of polarization. In dark after $V=V_B$, electron injection from Au electrodes is only possible in high voltage region , and this is supported by the appearance of peak C in Fig. 2a. The energy difference between Au work function (5.1 eV) and LUMO of pentacene is approximately 2.2 eV, and resulting energy barrier is sufficiently high for electron injection, and causes the third polarization peak in DCM. Some groups showed that eliminating extrinsic traps is one way for improving electron injection [41,42]. On the other hand, our finding in the present study showed that generation of free electrons by exciton dissociation provide another way to facilitate polarization reversal of P(VDF-TrFE) layer.

In contrast, CMS at the wavelengths of 630 nm and 670 nm (Figs. 4d and 4e) shows hysteresis loop in a way similar to electric field in pentacene layer shown in Fig. 2b. Results suggest that not only charge modulation but also electric-field modulation can be origins of the CMS intensity change. The spectrum shift induced by the field-modulation effect is given as $\Delta T = \frac{dT}{dE}\frac{1}{2}\alpha E^2$ where T is the transmission spectrum, E is the electric field and α is the

polarizing coefficient, indicating that the field-modulated spectrum fits to the first derivative curve of the absorption spectrum [43]. The first derivative of the optical absorption is plotted by a red dotted line in Fig. 3b. The first derivative curve of the optical absorption is in good agreement with the CMS data in the region between 600 nm and 700 nm where Davydov states of pentacene dominates the spectrum. In other words, Davydov states in the diode is modulated by the electric field produced by the spontaneous polarization, but this electric field contribution to free carrier generation for turn-over of polarization is limited. It is noteworthy that excitons separation by electric field depends on associated energy states [44]. In pentacene, excitons on E1 and E2 states are ready to separate into free electrons and holes while excitons on E3 and E4 is stably bounded. In pentacene/P(VDF-TrFE) diodes, spontaneous polarization of ferroelectric layer provides electrostatic field for excitons separation. Consequently, excitons on E1 and E2 states efficiently separate into free carriers whereas excitons separation from E3 and E4 states are limited.

Lastly, it is instructive to discuss hysteresis carrier behavior in the diode based on CMS measurement. In our previous study, we employed CMS measurement to probe carrier energetics in metal-insulator-semiconductor (MIS) type diode, i.e., Au/TIPS-pentacene/polyimide/ITO diode without ferroelectricity [45]. The MIS diode showed hysteresis behavior in C-V measurement, when high voltage ($|V|$>10 V) is applied. CMS

showed that the interfacial carriers Q_s in TIPS-pentacene changed as $\Delta Q_s(\propto -\Delta R/R) = C'_2 \Delta V$ (C'_2: capacitance of polyimide layer) in low voltage region whereas $\Delta Q_s = 0$ in high voltage region. This result indicated that holes at TIPS-pentacene/PI interface mainly occupied highest occupied molecular orbital (HOMO) of the TIPS-pentacene molecule in low voltage region, while holes further inject from TIPS-pentacene HOMO level into trap states in PI in high voltage region. That is, the creation of the trapped charges is a cause of hysteresis loops in the C-V characteristics of TIPS-pentacene/PI diode. On the contrary, in this study on Au/pentacene/P(VDF-TrFE)/ITO diode with ferroelectric P(VDF-TrFE) layer, CMS signal changed on keeping the relationship $-\Delta R/R \propto \Delta Q_s = C_2 \Delta V$ in the voltage region studied, indicating that carrier creation and accumulation always happen in pentacene layer, not in P(VDF-TrFE) layer. We conclude that hysteresis behavior in Au/pentacene/P(VDF-TrFE)/ITO diode was caused due to the turn-over of spontaneous polarization of P(VDF-TrFE). Note that both carrier trapping and polarization reversal lead to hysteresis behavior in the conventional I-V and C-V electrical measurements. On the other hand, CMS studies of MIS and MFS diodes demonstrate that the CMS technique is available to optically discriminate an origin of hysteresis behaviors in organic diodes, by directly probing carrier energetics that account for the observed hysteresis phenomena.

4. Conclusion

By using EFISHG measurement and CMS, we analyzed the carrier behaviors in ITO/P(VDF-TrFE)/pentacene/Au diodes. Results obtained by the DCM and EFISHG measurement showed that accumulated charge at the pentacene/P(VDF-TrFE) interface made a significant contribution to polarization reversal in the P(VDF-TrFE) layer and the process of polarization reversal differs between in dark and under light illumination conditions, owing to the photo carriers generated in the pentacene layer. In addition, CMS suggested that the injected carriers occupy and eliminate the molecular energy states of the pentacene layer in response to the polarization reversal of the P(VDF-TrFE) layer, and the light illumination assists electron accumulation for turn-over of spontaneous polarization. CMS coupled with EFISHG measurement is very effective for studying the carrier energetics of the organic semiconductor layer in organic devices based on thin ferroelectric polymer films.

References

[1] G. Meller and T. Grasser, *Organic Electronics*. Heidelberg: Springer, 2010.

[2] A. Köhler and H. Bässler, *Electronic processes in organic semiconductors*. Weinheim: Wiley-VCH, 2015.

[3] H. Klauk, *Organic Electronics*. Weinheim: Wiley-VCH, 2006.

[4] M. Pope and C. E. Swenberg, *Electronic Processes in Organic Crystals and Polymers*. New York: Oxford University Press, 1999.

[5] M. A. Lampert and P. Mark, *Current injection in solids*. New York: Academic Press, 1970.

[6] M. Iwamoto, T. Manaka, and D. Taguchi, "Modeling and visualization of carrier motion in organic films by optical second harmonic generation and Maxwell-displacement current," *J. Phys. D. Appl. Phys.*, vol. 48, no. 37, p. 373001, Sep. 2015.

[7] M. Iwamoto, T. Manaka, T. Yamamoto, and E. Lim, "Probing motion of electric dipoles and carriers in organic monolayers by Maxwell Displacement Current and optical second harmonic generation," *Thin Solid Films*, vol. 517, no. 4, pp. 1312–1316, 2008.

[8] E. Lim, T. Manaka, and M. Iwamoto, "Analysis of pentacene field-effect transistor with contact resistance as an element of a Maxwell-Wagner effect system," *J. Appl. Phys.*, vol. 104, no. 5, p. 54511, 2008.

[9] D. Taguchi, L. Zhang, J. Li, M. Weis, T. Manaka, and M. Iwamoto, "Analysis of Carrier Transients in Double-Layer Organic Light Emitting Diodes by Electric-Field-Induced Second-Harmonic Generation Measurement," *J. Appl. Phys.*, vol. 114, no. 35, pp. 15136–15140, 2010.

[10] R. Tamura, E. Lim, T. Manaka, and M. Iwamoto, "Analysis of pentacene field effect

transistor as a Maxwell-Wagner effect element," *J. Appl. Phys.*, vol. 100, no. 11, p. 114515, 2006.

[11] Y. Mashiko, D. Taguchi, M. Weis, T. Manaka, and M. Iwamoto, "The Maxwell-Wagner model for charge transport in ambipolar organic field-effect transistors: The role of zero-potential position," *Appl. Phys. Lett.*, vol. 101, no. 24, p. 243302, 2012.

[12] M. Weis, J. Lin, D. Taguchi, T. Manaka, and M. Iwamotoy, "The charge transport in organic field-effect transistor as an interface charge propagation: The maxwell-wagner effect model and transmission line approximation," *Jpn. J. Appl. Phys.*, vol. 49, no. 7 PART 1, pp. 0716031–0716038, 2010.

[13] J. C. Maxwell, *Electricity and magnetism*. New York: Dover publications, 1954.

[14] T. Manaka, E. Lim, R. Tamura, and M. Iwamoto, "Direct imaging of carrier motion in organic transistors by optical second-harmonic generation," *Nat. Photonics*, vol. 1, no. 10, pp. 581–584, 2007.

[15] E. Lim, T. Manaka, and M. Iwamoto, "Analysis of carrier injection into a pentacene field effect transistor by optical second harmonic generation measurements," *J. Appl. Phys.*, vol. 101, no. 2, p. 24515, 2007.

[16] K. Asadi, D. M. de Leeuw, B. de Boer, and P. W. M. Blom, "Organic non-volatile memories from ferroelectric phase-separated blends.," *Nat. Mater.*, vol. 7, no. 7, pp.

547–550, 2008.

[17] Y. Yuan, T. J. Reece, P. Sharma, S. Poddar, S. Ducharme, A. Gruverman, Y. Yang, and J. Huang, “Efficiency enhancement in organic solar cells with ferroelectric polymers,” *Nat. Mater.*, vol. 10, no. 4, pp. 296–302, 2011.

[18] Y. J. Park, I. S. Bae, S. Ju Kang, J. Chang, and C. Park, “Control of thin ferroelectric polymer films for non-volatile memory applications,” *IEEE Trans. Dielectr. Electr. Insul.*, vol. 17, no. 4, pp. 1135–1163, 2010.

[19] R. C. G. Naber, B. de Boer, P. W. M. Blom, and D. M. de Leeuw, “Low-voltage polymer field-effect transistors for nonvolatile memories,” *Appl. Phys. Lett.*, vol. 87, no. 20, p. 203509, 2005.

[20] H. Sakai, Y. Takahashi, and H. Murata, “Organic field effect transistors with dipole-polarized polymer gate dielectrics for control of threshold voltage,” *Appl. Phys. Lett.*, vol. 91, no. 11, p. 113502, 2007.

[21] R. C. G. Naber, C. Tanase, P. W. M. Blom, G. H. Gelinck, A. W. Marsman, F. J. Touwslager, S. Setayesh, and D. M. de Leeuw, “High-performance solution-processed polymer ferroelectric field-effect transistors,” *Nat. Mater.*, vol. 4, no. 3, pp. 243–248, 2005.

[22] R. Kalbitz, R. Gerhard, and D. M. Taylor, “Fixed negative interface charges compromise

organic ferroelectric field-effect transistors," *Org. Electron. physics, Mater. Appl.*, vol. 13, no. 5, pp. 875–884, 2012.

[23] M. Iwamoto and T. Manaka, "Probing and modeling of carrier motion in organic devices by optical second harmonic generation," *Thin Solid Films*, vol. 519, no. 3, pp. 961–963, 2010.

[24] J. Li, D. Taguchi, W. OuYang, T. Manaka, and M. Iwamoto, "Interaction of interfacial charge and ferroelectric polarization in a pentacene/poly(vinylidene fluoride-trifluoroethylene) double-layer device," *Appl. Phys. Lett.*, vol. 99, no. 6, p. 063302, 2011.

[25] X. Cui, D. Taguchi, T. Manaka, and M. Iwamoto, "Analysis of carrier behavior in C60/P(VDF-TrFE) double-layer capacitor by using electric-field-induced optical second-harmonic generation measurement," *J. Appl. Phys.*, vol. 114, no. 23, p. 234504, 2013.

[26] X. Cui, D. Taguchi, T. Manaka, W. Pan, and M. Iwamoto, "Study of effect of inserted pentacene layer in ITO/P(VDF-TrFE)/α-NPD/Au capacitor using electric-field-induced optical second-harmonic generation and displacement current," *Org. Electron.*, vol. 15, no. 2, pp. 537–542, Feb. 2014.

[27] M. Weis, J. Li, D. Taguchi, T. Manaka, and M. Iwamoto, "Effect of photogenerated

carriers on ferroelectric polarization reversal," *Appl. Phys. Express*, vol. 4, no. 12, p. 121601, 2011.

[28] J. H. Burroughes, C. A. Jones, and R. H. Friend, "New semiconductor device physics in polymer diodes and transistors," *Nature*, vol. 335, pp. 137–141, 1988.

[29] P. J. Brown, H. Sirringhaus, M. Harrison, M. Shkunov, and R. H. Friend, "Optical spectroscopy of field-induced charge in self-organized high mobility poly(3-hexylthiophene)," *Phys. Rev. B*, vol. 63, no. 12, p. 125204, Mar. 2001.

[30] T. Verbiest, K. Clays, and V. Rodriguez, *Second-Order Nonlinear Optical Characterization Techniques*. Boca Raton: CRC Press, 2009.

[31] X. Chen, D. Taguchi, T. Manaka, and M. Iwamoto, "Selective observation of photo-induced electric fields inside different material components in bulk-heterojunction organic solar cell," *Appl. Phys. Lett.*, vol. 104, no. 1, p. 013306, 2014.

[32] L. Zhang, D. Taguchi, J. Li, T. Manaka, and M. Iwamoto, "Probing of interfacial charging and discharging in double-layer devices with a polyimide blocking layer by time-resolved optical second harmonic generation," *J. Appl. Phys.*, vol. 108, no. 9, pp. 1–5, 2010.

[33] S. Yoshita, R. Tamura, D. Taguchi, M. Weis, E. Lim, T. Manaka, and M. Iwamoto, "Displacement current analysis of carrier behavior in pentacene field effect transistor

with poly(vinylidene fluoride and tetrafluoroethylene) gate insulator", *J. Appl. Phys.*, vol. 106, no. 2, p. 024505, July 2009.

[34] Z. Shi, D. Taguchi, T. Manaka, and M. Iwamoto, "Observation of turnover of spontaneous polarization in ferroelectric layer of pentacene/poly-(vinylidene-trifluoroethylene) double-layer capacitor under photo illumination by optical second-harmonic generation measurement," *J. Appl. Phys.*, vol. 119, no. 16, p. 165502, 2016.

[35] T. Manaka, S. Kawashima, and M. Iwamoto, "Charge modulated reflectance topography for probing in-plane carrier distribution in pentacene field-effect transistors," *Appl. Phys. Lett.*, vol. 97, no. 11, pp. 1–4, 2010.

[36] J. Li, D. Taguchi, W. Ouyang, T. Manaka, and M. Iwamoto, "Interaction of interfacial charge and ferroelectric polarization in a pentacene/poly(vinylidene fluoride-trifluoroethylene) double-layer device," *Appl. Phys. Lett.*, vol. 99, no. 6, pp. 3–5, 2011.

[37] A. F. Prikhotko, A. F. Skorobogatko, and L. I. Tsikora, "Spectral investigations of pentacene crystals," *Opt. Spectrosc.*, vol. 26, p. 524, 1969.

[38] L. Sebastian, G. Weiser, and H. Bässler, "Charge transfer transitions in solid tetracene and pentacene studied by electroabsorption," *Chem. Phys.*, vol. 61, no. 1–2, pp. 125–135,

Oct. 1981.

[39] O. Ostroverkhova, S. Shcherbyna, D. G. Cooke, R. F. Egerton, F. A. Hegmann, R. R. Tykwinski, S. R. Parkin, and J. E. Anthony, “Optical and transient photoconductive properties of pentacene and functionalized pentacene thin films: Dependence on film morphology,” *J. Appl. Phys.*, vol. 98, no. 3, p. 033701, 2005.

[40] M. W. B. Wilson, A. Rao, B. Ehrler, and R. H. Friend, “Singlet exciton fission in polycrystalline pentacene: from photophysics toward devices.,” *Acc. Chem. Res.*, vol. 46, no. 6, pp. 1330–8, Jun. 2013.

[41] M. Ahles, R. Schmechel, and H. Von Seggern, “N-type organic field-effect transistor based on interface-doped pentacene,” *Appl. Phys. Lett.*, vol. 85, no. 19, pp. 4499–4501, 2004.

[42] T. Yasuda, T. Goto, K. Fujita, and T. Tsutsui, “Ambipolar pentacene field-effect transistors with calcium source-drain electrodes,” *Appl. Phys. Lett.*, vol. 85, no. 11, pp. 2098–2100, 2004.

[43] M. Cardona, *Modulation Spectroscopy*. London: Academic Press, 1969.

[44] E. A. Silinsh, A. I. Belkind, D. R. Balode, A. J. Biseniece, V. V. Grechov, L. F. Taure, M. V. Kurik, J. I. Vertzymacha, I. Bok, "Photoelectrical properties, energy level spectra, and photogeneration mechanism of pentacene," *Phys. Stat. Sol. (a)*, vol.

25, pp. 339-347, 1974.

[45] E. Lim, D. Taguchi, and M. Iwamoto, “Analysis of carrier transport and carrier trapping in organic diodes with polyimide-6,13-Bis(triisopropylsilylethynyl)pentacene double-layer by charge modulation spectroscopy and optical second harmonic generation measurement,” *Appl. Phys. Lett.*, vol. 105, no. 7, p. 073301, Aug. 2014.

Figure captions

Figure 1: (a) Device structure of ITO/P(VDF-TrFE)/pentacene/Au diode used here and experimental setup for EFISHG measurement. (b) A model of ITO/P(VDF-TrFE)/pentacene/Au diode taking account of interfacial charges Q_s and spontaneous polarization P, on the basis of Maxwell-Wagner effect. (c) Experimental setup for CMS measurement.

Figure 2: DCM measurement (a) and EFISHG measurement result (b) for the ITO/ P(VDF-TrFE)/pentacene/Au diode in dark and under light illumination. The arrows denote the voltage sweep direction. (c) Charge Q_s accumulated at the pentacene/P(VDF-TrFE) interface under illumination, obtained from the EFISHG result.

Figure 3: CMS spectrum (-$\Delta R/R$) for the ITO/ P(VDF-TrFE)/pentacene/Au diode. The relative change in the reflection spectrum was measured in the forward sweep (-60 V to +60 V) in respect to the reference spectrum at $V = -60$ V (a), and in the backward sweep (+60 V to -60 V) with reference to $V = +60$ V (b).

Figure 4: (a) Absorption spectrum of pentacene. The inset illustrates the energy diagram for optical transitions in pentacene. (b-e) The voltage dependence of the CMS at the wavelength of (b) 540 nm, (c) 580 nm, (d) 630 nm, and (e) 670 nm, corresponding to optical absorption peak of the pentacene film.

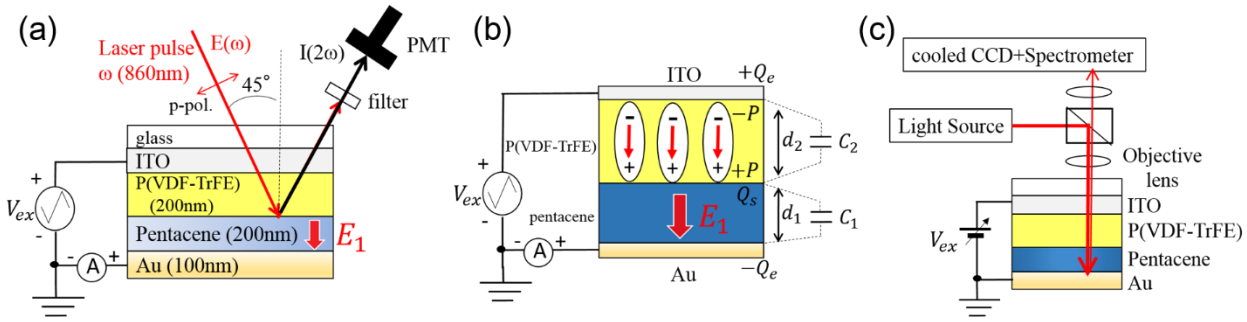

Fig. 1: T. Otsuka et al.

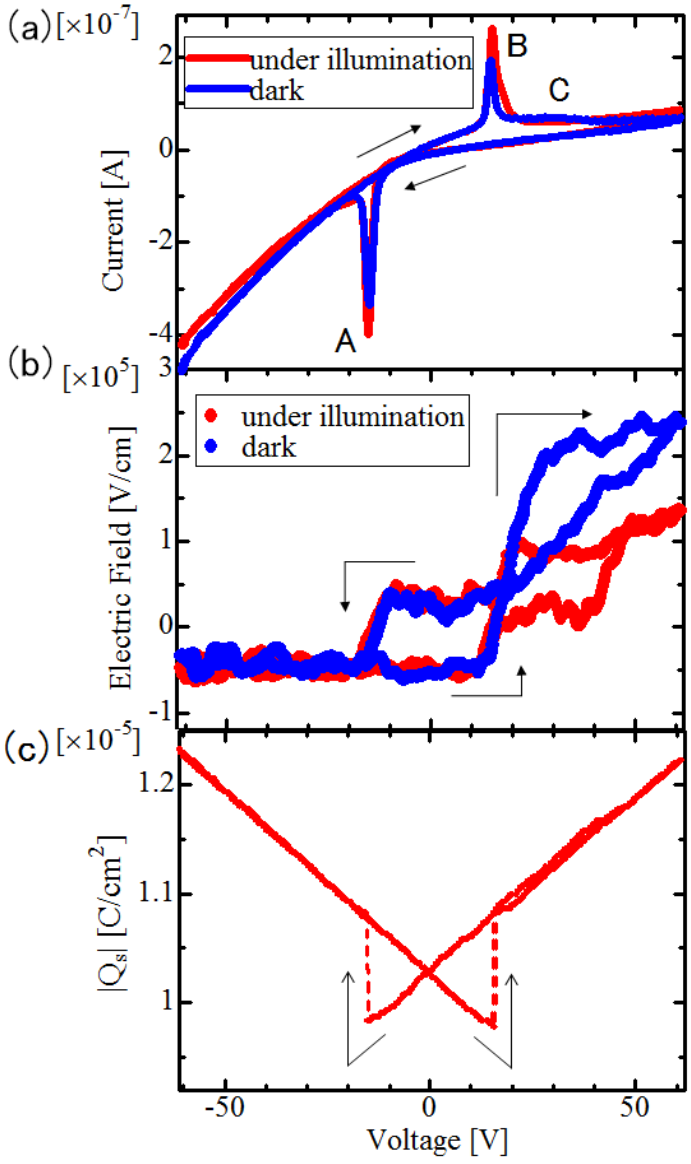

Fig. 2: T. Otsuka et al.

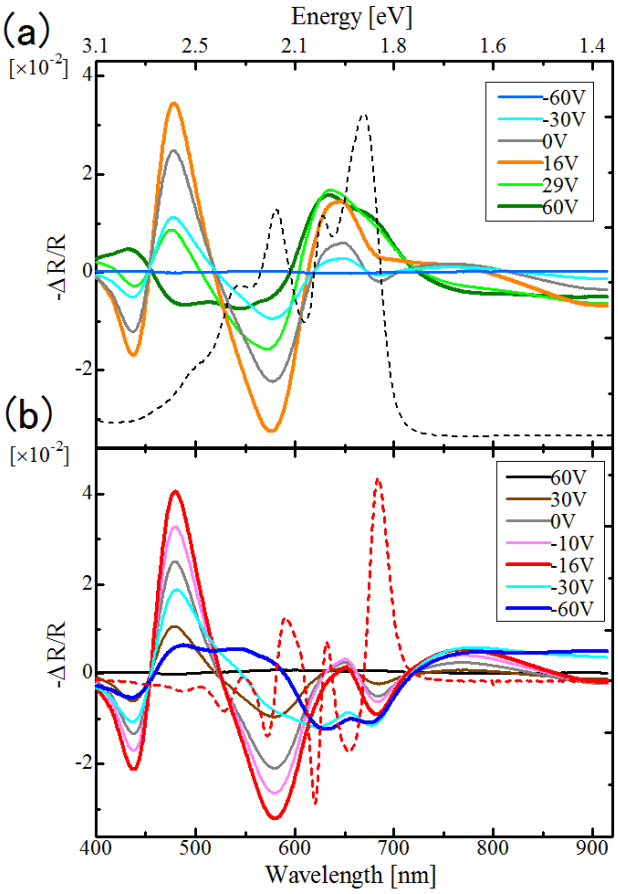

Fig. 3: T. Otsuka et al.

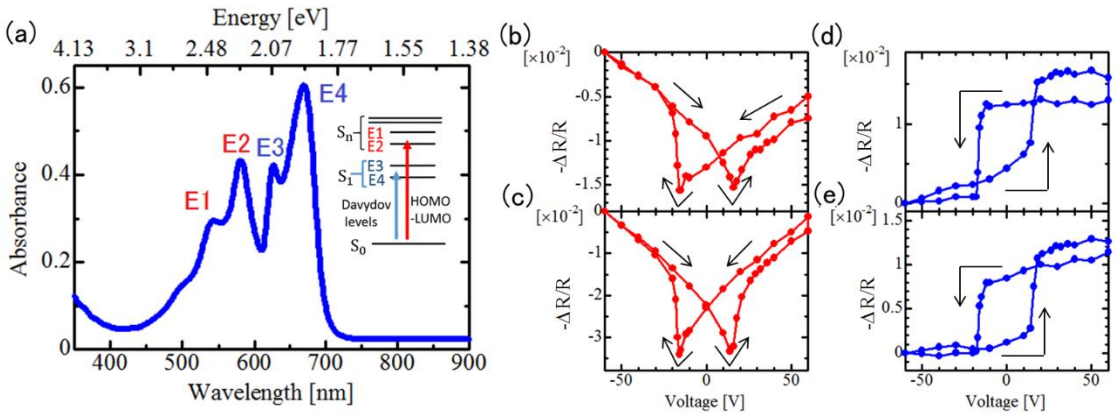

Fig. 4: T. Otsuka et al.